Polymer 50 (2009) 462–466

Contents lists available at ScienceDirect

Polymer

journal homepage: www.elsevier.com/locate/polymer

Preparation of Au and Au–Pt nanoparticles within PMMA matrix using UV and X-ray irradiation

Eda Ozkaraoglu, Ilknur Tunc, Sefik Suzer*

Department of Chemistry and Institute of Materials and Nanotechnology, Bilkent University, 06800 Ankara, Turkey

ARTICLE INFO

Article history:
Received 6 October 2008
Received in revised form
28 November 2008
Accepted 3 December 2008
Available online 9 December 2008

Keywords:
Photoreduction and photo-patterning
Nucleation and growth
X-ray photoelectron spectroscopy

ABSTRACT

Au and Au–Pt alloy nanoparticles are prepared and patterned at room temperature within the PMMA polymer matrix by the action of 254 nm UV light or X-rays. The polymer matrix enables us to entangle the kinetics of the photochemical reduction from the nucleation and growth processes, when monitored by UV–vis spectroscopy. Accordingly, increase of the temperature to 50 °C of the reaction medium increases the nucleation and growth rates of the nanoparticle formation by more than one order of magnitude, due to enhanced diffusion and nucleation at the higher temperature, but has no effect on the photochemical reduction process. Presence of Pt ions also increases the same rate, but by a factor two only. Similar photochemical reduction and particle growth take also place within the PMMA matrix, when these metal ions are subjected to prolonged exposure to X-rays, as evidenced by XPS analysis. Both angle-resolved and charge-contrast measurements using XPS reveal that the resultant Au and Pt species are in close proximity to each other, indicating the Au–Pt alloy formation to be the most likely case.

1. Introduction

Metallic nanoparticles have attracted a great deal of attention since they lead to many size-dependent, electrical, magnetic, chemical, and optical properties [1]. Bimetallic nanoparticles are particularly more important than their monometallic counterparts in the field of catalysis because of their enhanced activity [2–5]. The structure of bimetallic materials mainly depends on preparation conditions. Hirai reported an extensive study on synthesis Au–Pt bimetallic nanoparticles in aqueous and nonaqueus reaction media by using different types of stabilizer [6]. The concentration dependent changes in morphology for a series of Au–Pt bimetallic nanoparticles were discussed by Chen et al. [7]. Garcia-Gutierrez synthesized Au–Pt bimetallic nanoparticles by polyol method and stabilized them with poly(vinyl-pyrolidone), modifying the synthesis temperature [8]. Luo and coworkers reported on controlling composition and phase properties of carbon-supported Au–Pt bimetallic nanoparticles [9,10]. Water soluble size and composition controlled Au–Pt nanoparticles were also synthesized recently by the same group, who also reported on an enhanced catalytic activity towards the nanoparticle formation due to the presence of Pt ions [11,12].

Interest in metal particles–polymer systems is also accelerating due to their various technological applications [13–15]. In this regard, Faupel et al. prepared Ni, Cu, Ag, and Au nanoparticles on polymers (polyimide, polystyrene, Teflon, PMDA–ODA) with different compositions [16–19]. Synthesis of metallic nanoparticles within polymeric media using photochemical means is an attractive route due to the relative simplicity of the technique and the possibility to combine with widely used lithographic methods [20–25]. However, in all of these synthesis methods elevated temperature(s) and/or certain photo-sensitizers were needed. On the other hand, we have recently presented a simple room temperature method for the preparation of monometallic Au nanoparticles using deep-UV and X-ray irradiation within poly(methyl methacrylate), PMMA, matrix [26,27]. Utilization of X-rays or energetic particles for the preparation of nanoparticles is particularly important for direct-writing and patterning applications using strong Synchrotron sources [28–31]. In this contribution we extend this study to formation of bimetallic Au–Pt nanoparticles within PMMA matrix, in order to further our understanding of the kinetics of the various processes involved. UV–vis and XPS techniques are used respectively, to entangle the kinetics of photoreduction and nucleation and particle growth processes, and to asses the structure of the Au and Pt particles produced within the polymer matrix.

2. Experimental section

$HAuCl_4$ (hydrogen tetrachloroaurate), H_2PtCl_6 (dihydrogen hexachloroplatinate), and PMMA (poly(methyl methacrylate))

* Corresponding author. Tel.: +90 312 2901476; fax: +90 312 2664579.
E-mail address: suzer@fen.bilkent.edu.tr (S. Suzer).

0032-3861/$ – see front matter © 2008 Elsevier Ltd. All rights reserved.
doi:10.1016/j.polymer.2008.12.008

with $M_w = 100.000$ were purchased from Aldrich, and used without further treatment. Solutions containing 6 mM Au ions or equal molar (3 mM) Pt and Au ions in 0.5% (w/v) PMMA in acetone, are cast and dried at room temperature to obtain self-standing films. Thickness of the polymer film is arbitrary but is chosen to give a clear record with UV–vis spectrum. Nanoparticles in PMMA matrix are produced by the action of the 254 nm deep-UV radiation, using a low pressure 10 W Hg lamp. Reduction of Au ions (using the absorption band around 320 nm) and subsequent nucleation and growth of Au–Pt nanoparticles (using the absorption band around 530 nm) are followed by Carry 5E UV–vis–NIR spectrophotometer. UV-patterning is accomplished on the films cast on Si substrates by using a Cu-mesh as the mask.

After complete photoreduction the film is introduced into the XPS spectrometer for further analysis. In a different set of experiments, the films are introduced into the XPS spectrometer for both inducing and also monitoring the reduction by X-rays. The XPS system is a Kratos ES300 spectrophotometer with Mg Kα (nonmonochromatized) source at 1253.6 eV, and operated at 120 W (15 kV at 8 mA). The data are recorded normally at 90° take-off angle, but for Angle Dependent XPS Analysis a smaller take-off angle (30°) is also used. For gathering further information about proximity of Au and Pt nanoparticles produced within the PMMA matrix, we have also performed charge-contrast XPS analysis, a method recently developed in our laboratory, where charging behavior of various XPS peaks in a composite surface structure are compared and contrasted [32]. The XPSPEAK 4.0 fitting program is used for deconvolution of the peaks.

3. Results

3.1. Au and bimetallic Au–Pt nanoparticle production within PMMA matrix

PMMA has been chosen because of its superior quality for microelectronic fabrication, and secondly in comparison with solution medium, the kinetics of various processes can be slowed down and entangled from each other as shown in Fig. 1 for the case of Au-only at room temperature and at 50 °C. Absorption band around 320 nm belongs distinctly to Au^{3+}, and production of Au nanoparticles can easily be followed by the surface plasmon band around 530 nm.

The overall process can be broken down into 3 separate elementary steps as *(i) photochemical reduction, (ii) nucleation, and (iii) growth.* Use of PMMA matrix enables us to easily separate the photochemical reduction process from the other two, as shown in Fig. 1, both at room temperature and at 50 °C. Whereas the rate of the photochemical reduction is not affected, as evidenced by the decrease in the intensity of the 320 nm band in time, the intensity of the SPR band around 530 nm increases drastically at the higher temperature due to the enhanced diffusion, nucleation, and growth.

When the same procedure is applied to the film containing equal molar Au and Pt salts, the features in the absorption bands do not change at all, since neither Pt ions nor Pt nanoparticles exhibit a discernible absorption band within the UV–vis–NIR region. However, to our surprise the presence of Pt ions within the matrix effects the nucleation and growth rate of the Au (or possibly Au–Pt alloy) nanoparticle formation, as summarized in Fig. 2, where the intensity of the Au SPR band is plotted against time in a logarithmic fashion for the cases of the film containing (i) Au ions at room temperature and at 50 °C, and (ii) Au:Pt ions also at these two different temperatures. Although, the presence of Pt ions has no measurable effect on the photoreduction rate, it increases the intensity of the SPR especially in the early times (1–20 min), hence, most likely, effects both the rates of the nucleation and particle growth processes.

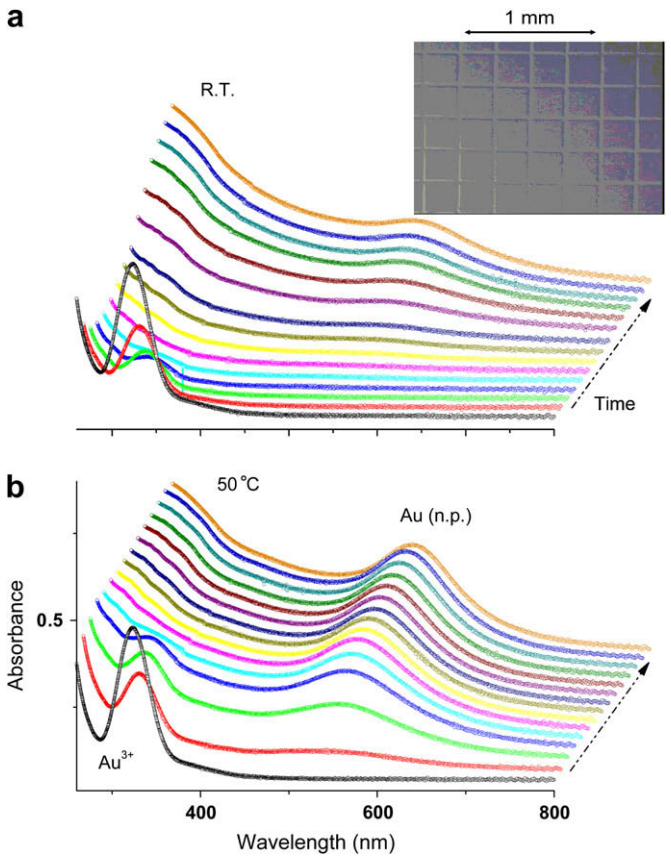

Fig. 1. A set of UV–vis–NIR spectra recorded in time for following the reduction of Au^{3+} ions and formation of Au nanoparticles within a PMMA film by 254 nm UV irradiation at room temperature (R.T.) (a), and at 50 °C (b). The absorption bands around 320 and 530 nm belong to the Au^{3+} ions and the Surface Plasmon Resonance (SPR) of the Au nanoparticles. The inset shows a photo-patterned film of PMMA using a Cu-mesh as the mask, where dark areas correspond to Au nanoparticles produced by the action of the UV irradiation.

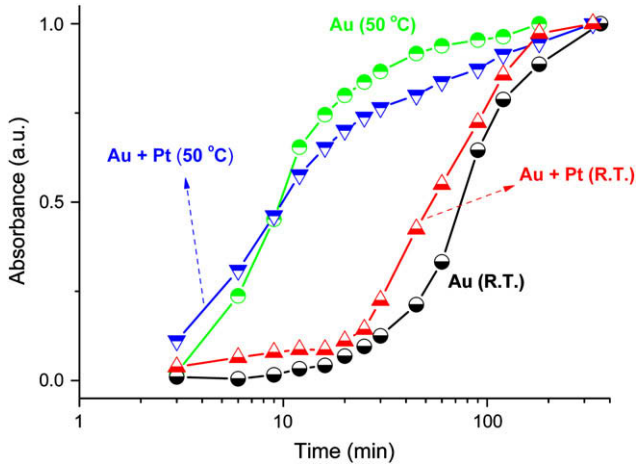

Fig. 2. Intensity of the SPR band of the Au nanoparticles around 530 nm, in the absence, and the presence of Pt ions, at two different temperatures, plotted against the logarithm of time. Experimental data are given as individual points, and the lines are the best fits (Table 1) using the Avrami equation.

3.2. Au and Au–Pt nanoparticle production with X-rays

As we had demonstrated in our previous papers, prolonged exposure to X-rays also leads to reduction of certain metal ions like Au^{3+} and Pt^{4+} to their neutral states, and if the conditions are favorable, these neutral particles aggregate and form nanoparticles as a result of their large cohesive energies, both within the polymer matrix and also on silicon substrates [26,27]. XPS is a suitable technique, since the reduction can be induced by the prolonged X-ray exposure, and the binding energy differences can be simultaneously monitored. For example, the binding energies of the corresponding $Au4f_{7/2}$ peaks are 87.5 eV and 85.5 eV for the Au^{3+} ion and neutral, isolated Au^0 atoms, respectively, at the beginning of the exposure, for the case of the polymer sample containing Au salt only (not shown) [26,27], as well as that containing Au and Pt salts together, as depicted in Fig. 3. As the exposure period is prolonged the intensity of the spin–orbit doublet corresponding to the ionic gold diminishes, and at the same time the binding energy of the neutral gold decreases towards the bulk value of the metal at 84.0 eV. The latter shift is related with the nucleation and particle growth as was reported by us and numerous other workers in the field [26,27,33–35]. As can also be gathered from Fig. 3, similar changes corresponding to reduction of the Pt^{4+} ions and nucleation and growth are observable in the Pt4f peaks. However, contrary to the case of Au, and in accord with our previous findings [27], complete reduction can not be achieved neither for the case of Pt-only nor Au–Pt mixtures, as also emphasized and shown in the last spectrum of Fig. 3, which corresponds to more than 24 h of X-ray exposure. In the final spectrum of the polymer sample, the gold 4f peaks result in a narrow spin–orbit doublet, but the Pt4f peaks are broad and can only be fitted to 2 spin–orbit doublets (see also Fig. 4), the lower energy of which can be assigned to Pt^0 and the higher one to positively charged Pt^{x+} moieties.

3.3. Angle-resolved XPS measurements of the Au–Pt nanoparticles

Since only limited information can be obtained from the position of the SPR band of the Au–Pt nanoparticles as to whether the particles are alloys or other structures like core–shell type, etc. we had also carried out Angle-Resolved XPS measurements as shown in Fig. 4, for the Au–Pt nanoparticles formed within the PMMA matrix at two different electron take-off angles [36]. If the structure of the particles was different from the simple spherical and homogeneously distributed alloy formation, it would have shown up as some changes in the relative intensities of the Au 4f and Pt 4f peaks, recorded at two different angles. As can be gathered from the figure, the absence of any significant difference at two angles supports our claim that the alloy formation is the nature of these nanoparticles.

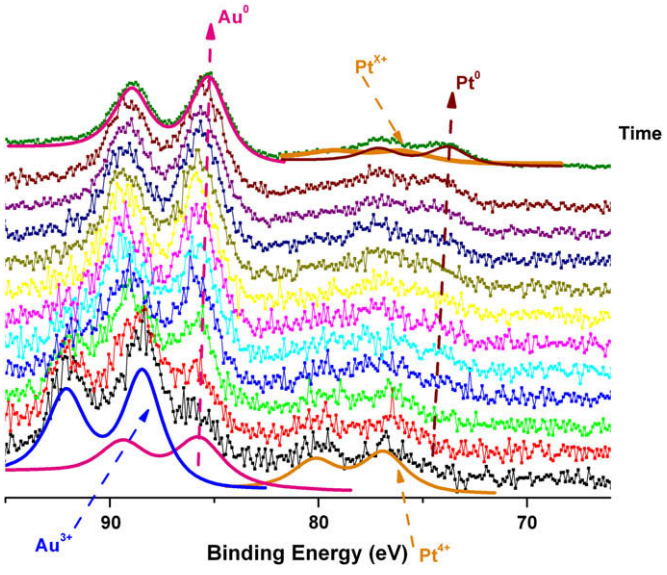

Fig. 3. A set of XPS spectra recorded in the course of a long X-ray exposure of the PMMA film containing Au and Pt salts together. Note that the intensity of the peaks corresponding to both Au^{3+} and Pt^{4+} ions diminishes in time and the peaks corresponding to both Au^0 and Pt^0 gain intensity and also shift gradually towards their bulk metallic values of 84.0 and 71.2 eV for Au and Pt respectively.

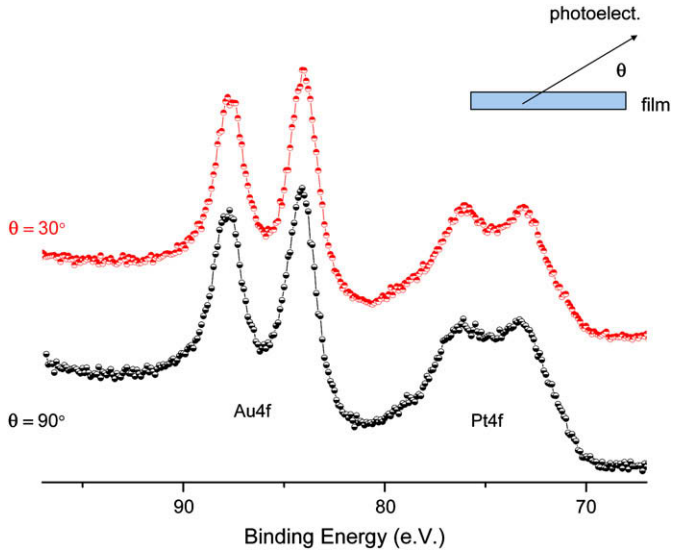

Fig. 4. Au and Pt 4f regions of the XPS spectrum of Au–Pt nanoalloys prepared within a PMMA film, recorded at two different electron take-off angles.

3.4. Charge-contrast XPS measurements of the Au–Pt nanoparticles

Measured binding energies are also susceptible to other factors like charging, especially in a non-conducting polymer matrix. Although charge compensation is the usual procedure practiced, we [32], and others [37] have been utilizing this charging for harvesting additional information about the samples analyzed. For example, by letting our sample charge more extensively via biasing the sample negatively, and tracking carefully the charging shifts of the various peaks, we obtain information about the proximity of the chemical species involved. Applying a negative bias to the sample repels the otherwise neutralizing low energy electrons falling on the sample and enhances the positive charging of the sample due to photoemission process (Scheme 1).

In Fig. 5(a), we depict the C1s region of a PMMA sample containing Au and Pt ions after UV photochemical reduction. When the

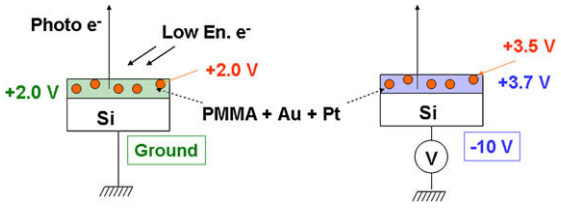

Scheme 1. Schematic representation of the potentials measured by XPS, in different species of the PMMA film containing the photoreduced Au and Pt ions together, when the sample is grounded and under −10 V bias.

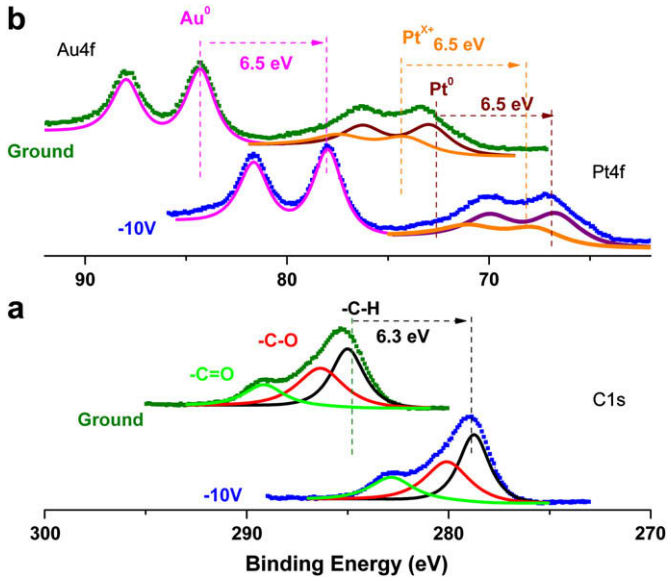

Fig. 5. (a) C1s spectra of the PMMA containing UV-reduced Au and Pt ions, recorded when the sample is grounded and subjected to −10 V bias. (b) Au4f and Pt4f regions again recorded when the sample is grounded and subjected to −10 V bias.

sample is grounded, the C1s peaks appear at 2.0 eV higher binding energy (lower kinetic energy) due to partial positive charging of the sample. After application of −10 V, the three C1s peaks of the PMMA matrix all shift to a −6.3 eV lower binding energy (higher kinetic energy), instead of the full −10 eV expected, due to enhanced charging of the sample, as a result of repelling of the low energy electrons. Hence, the −10 V applied introduces an additional +1.7 eV voltage increase on the sample, such that all together the sample exhibits +3.7 eV charging shift. The purpose of this exercise is actually related with assessing whether or not similar shifts are observable in Au and Pt 4f peaks. The outcome, as shown in Fig. 5(b), is that both the single Au4f spin–orbit doublet, and the two Pt4f doublets (belonging to the neutral as well as ionic moieties) undergo a slightly different shift of 6.5 eV, which is 0.2 eV different from the C1s peaks, but exactly the same amount for all Au and Pt moieties. This leads us to conclude that the resultant photoreduced Au, and Pt, as well as the partially photoreduced Pt species are within the proximity of each other, possibly as Au–Pt alloy particles containing some unreduced Pt ions.

4. Discussion and conclusions

Keeping in mind that, that nanoparticles below 2 nm size do not exhibit any measurable SPR band, and that the photochemical reduction is completed at the very early stages, our kinetic data revealed by the UV–vis measurements can only be related to diffusion and particle growth. One can use Avrami's model [38] which is often used for crystallization and growth kinetics, as recently applied by Njoki et al. for the assessment of the catalytic effect of the pre-synthesized Pt particles on the kinetics of the formation of Au nanoparticles [11,12]. Adopting their approach, we can relate the increase in the intensity (absorbance) of the SPR band with time as:

$$A = C^*[1 - \exp(-k^*t^n)]$$

where, A is the absorbance of the SPR band, C is the proportionality constant, k is the overall rate constant and, n is the critical growth exponent. Under diffusion controlled mass-flow conditions, a critical exponent of 2.5 or less has been reported for thermal nucleation [39]. Accordingly, Njoki et al. found that values very close to 2 fitted best to their kinetic data, and suggested that thermal nucleation and three-dimensional growth processes are operative. Therefore, we kept $n = 2$ and fitted the four sets of data shown in Fig. 2 to obtain the best fits to the rate constant k as given in Table 1. We see that the largest effect is the temperature. The rate constant k increases from 1.3×10^{-4} to 76×10^{-4} going from the R.T. to 50 °C, causing more than one order of magnitude increase in the rate constant, and the presence of Pt causes only a factor of two increase on k (going from 1.3×10^{-4} to 2.3×10^{-4}). Since the effect of the temperature is overwhelmingly large, the effect of the presence of Pt on k is measurable but not so significant at 50 °C.

The large factor imparted by the temperature increase is expected since the heating not only increases the diffusion rate of the neutral atoms formed within the polymer matrix, but also decreases the energetic barrier size to critical nucleus formation (ΔG^*), as recently discussed [40,41]. For the effect of the Pt ions, several mechanisms are possible and may be speculated. In the previously mentioned work of Njoki et al., 12 Pt–H species formed on the surface of pre-synthesized Pt nanoparticles were presented to be responsible for the increased rate of Au reduction, thus Au nanoparticle formation. In our case, the photochemical reduction is well separated in time from the nucleation and growth processes. Furthermore, it was observed that Pt doesn't affect the reduction rate of gold ions. Hence, the increase in the rates, both in UV and also in X-ray induced production (not shown), may be related to the basic nucleation requirements, since it is suspected that Pt helps Au to overcome the critical nucleus formation step and thereby increases the nucleation rate of the Au–Pt bimetallic nanoparticles.

We must also point out that we are quite aware of the fact that, when comparing the kinetics of nanoparticle formation, the effect(s) of the medium (aqueous, non-aqueous, polymer, or glass matrix, etc.) must be adequately sorted out. However, as we have tried to bring out in this work, there seems to be certain characteristics of these ions (and subsequently the nanoparticles formed), like catalytical effect of Pt ions, electrochemical reduction potentials, etc., which are apparently independent of the medium used [11,12,42].

As the main conclusion of this work, we have shown that by carrying out the photochemical production of Au and Au–Pt nanoparticles within the PMMA polymeric matrix, the kinetics of the various processes involved can be entangled and monitored using UV–vis–NIR spectroscopic technique. Angle-Resolved and Charge-Contrast XPS measurements enabled us to claim that the resultant particles most probably have Au–Pt alloy-like structure. Although not mentioned in this work, but brought out in our previous work, additives can easily be incorporated into polymeric matrices for sensitizing and/or quenching some of the processes involved, for bettering the desired properties of the finished products [43]. Better understanding of the kinetics and other physicochemical factors will lead to better control of size, shape, and composition of nanoparticles, which eventually will lead to better control of their usage, not only in photo-patterning and

Table 1
Calculated Avrami rate constants for nucleation and growth of nanoparticles following photochemical reduction within the PMMA matrix.

Sample	k	n
Au (R.T.)	0.00013	2
Au (50 °C)	0.0076	2
Au–Pt (R.T.)	0.00025	2
Au–Pt (50 °C)	0.0082	2

direct-writing, but also in catalytic, sensing, drug delivery, and other important applications.

Acknowledgements

This work was partially supported by TUBA (Turkish Academy of Sciences) and TUBITAK (The Scientific and Technological Research Council of Turkey) through the Grant no. 106T409.

References

[1] El-Sayed MA. Accounts of Chemical Research 2001;34:257.
[2] Haruta M. Catalysis Today 1997;36:153.
[3] Maye MM, Lou YB, Zhong CJ. Langmuir 2000;16:7520.
[4] Lou YB, Maye MM, Han L, Luo J, Zhong CJ. Chemical Communications 2001:473.
[5] Zhong CJ, Maye MM. Advanced Materials 2001;13:1507.
[6] Hirai H. Formation and catalytic functionality of synthetic polymer–noble metal colloid, vol. 13. Taylor & Francis; 1979. p. 633.
[7] Chen HM, Peng HC, Liu RS, Hu SF, Jang LY. Chemical Physics Letters 2006;420:484.
[8] Garcia-Gutierrez DI, Gutierrez-Wing CE, Giovanetti L, Ramallo-Lopez JM, Requejo FG, Jose-Yacaman M. Journal of Physical Chemistry B 2005;109:3813.
[9] Luo J, Maye MM, Petkov V, Kariuki NN, Wang LY, Njoki P, et al. Chemistry of Materials 2005;17:3086.
[10] Luo J, Njoki PN, Lin Y, Mott D, Wang LY, Zhong CJ. Langmuir 2006;22:2892.
[11] Njoki PN, Jacob A, Khan B, Luo J, Zhong CJ. Journal of Physical Chemistry B 2006;110:22503.
[12] Njoki PN, Luo J, Wang LY, Maye MM, Quaizar H, Zhong CJ. Langmuir 2005;21:1623.
[13] Pandey P, Datta M, Malhotra BD. Analytical Letters 2008;41:159.
[14] Kogan MJ, Olmedo I, Hosta L, Guerrero AR, Cruz LJ, Albericio F. Nanomedicine 2007;2:287.
[15] Wong CPE. Polymers for electronic and photonic applications. Boston: Academic Press; 1993.
[16] Zaporojtchenko V, Strunskus T, Behnke K, Von Bechtolsheim C, Thran A, Faupel F. Microelectronic Engineering 2000;50:465.
[17] Zaporojtchenko V, Strunskus T, Behnke K, Von Bechtolsheim C, Kiene M, Faupel F. Journal of Adhesion Science and Technology 2000;14:467.
[18] Zaporojtchenko V, Zekonyte J, Biswas A, Faupel F. Surface Science 2003; 532:300.
[19] Zaporojtchenko V, Zekonyte J, Wille S, Schuermann U, Faupel F. Nuclear Instruments and Methods in Physics Research Section B – Beam Interactions with Materials and Atoms 2005;236:95.
[20] Tanaka H, Mitsuishi M, Miyashita T. Langmuir 2003;19:3103.
[21] Korchev AS, Bozack MJ, Slaten BL, Mills G. Journal of the American Chemical Society 2004;126:10.
[22] Alexandrov A, Smirnova L, Yakimovich N, Sapogova N, Soustov L, Kirsanov A, et al. Applied Surface Science 2005;248:181.
[23] Yin DH, Horiuchi S, Morita M, Takahara A. Langmuir 2005;21:9352.
[24] Pal A, Esumi K, Pal T. Journal of Colloid Interface Science 2005;288:396.
[25] Cen L, Neoh KG, Cai Q, Kang ET. Journal of Colloid Interface Science 2006; 300:190.
[26] Karadas F, Ertas G, Ozkaraoglu E, Suzer S. Langmuir 2005;21:437.
[27] Ozkaraoglu E, Tunc I, Suzer S. Surface and Coatings Technology 2007; 201:8202.
[28] Ma Q, Moldovan N, Mancini DC, Rosenberg RA. Applied Physics Letters 2000; 76:2014.
[29] Yang YC, Wang CH, Hwu YK, Je JH. Materials Chemistry and Physics 2006;100:72.
[30] Wang CH, Hua TE, Chien CC, Yu YL, Yang TY, Liu CJ, et al. Materials Chemistry and Physics 2007;106:323.
[31] Wang CH, Chien CC, Yu YL, Liu CJ, Lee CF, Chen CH, et al. Journal of Synchrotron Radiation 2007;14:477.
[32] Suzer S, Dana A, Ertas G. Analytical Chemistry 2007;79:183.
[33] Luo K, Kim DY, Goodman DW. Journal of Molecular Catalysis A – Chemical 2001;167:191.
[34] Choudhary TV, Goodman DW. Topics in Catalysis 2002;21:25.
[35] Ohgi T, Fujita D. Physical Review B 2002;66.
[36] Briggs D, Seah MP. Practical surface analysis. Chichester: Wiley; 1999.
[37] Dubey M, Gouzman I, Bernasek SL, Schwartz J. Langmuir 2006;22:4649.
[38] Avrami M. The Journal of Chemical Physics 1940;8:212.
[39] Exarhos GJ, Aloi MJ. Thin Solid Films 1990;193:42.
[40] Kulkarni AM, Zukoski CF. Langmuir 2002;18:3090.
[41] Smorodin VY, Hopke PK. Journal of Physical Chemistry B 2004;108:9147.
[42] Suzer S. Journal of Electron Spectroscopy and Related Phenomena 2001; 114:1151.
[43] Balci S, Birer O, Suzer S. Polymer 2004;45:7123.